

***Searching for Molecular Solutions* – FIGURE COLOR VERSIONS**

This File contains a subset of the figures published within *Searching for Molecular Solutions* which are considered to be enhanced further when rendered in color. Most (but not all) of these are protein or nucleic structural images and diagrams. In some cases, more informational detail is also provided within the Figure itself.

Contents:

Chapter	<i>Searching for Molecular Solutions</i> Page Number	Page Number for this File	Figure
<u>2</u>	50	3	<u>2.2</u>
<u>3</u>	69	5	<u>3.1</u>
<u>3</u>	70	6	<u>3.2</u>
<u>3</u>	76	8	<u>3.4</u>
<u>3</u>	77	10	<u>3.5</u>
<u>3</u>	96	12	<u>3.7</u>
<u>4</u>	134	13	<u>4.9</u>
<u>4</u>	136	15	<u>4.10</u>
<u>5</u>	150	17	<u>5.1</u>
<u>5</u>	156	19	<u>5.2</u>
<u>5</u>	160	20	<u>5.3</u>
<u>5</u>	161	21	<u>5.4</u>

5	176	22	5.6
5	183	23	5.10
6	190	25	6.1
6	209	27	6.7
7	237	29	7.1
7	241	31	7.3
7	247	32	7.5
7	256	33	7.9
8	293	34	8.5
9	338	36	9.7
10	359	38	10.2

CHAPTER 2

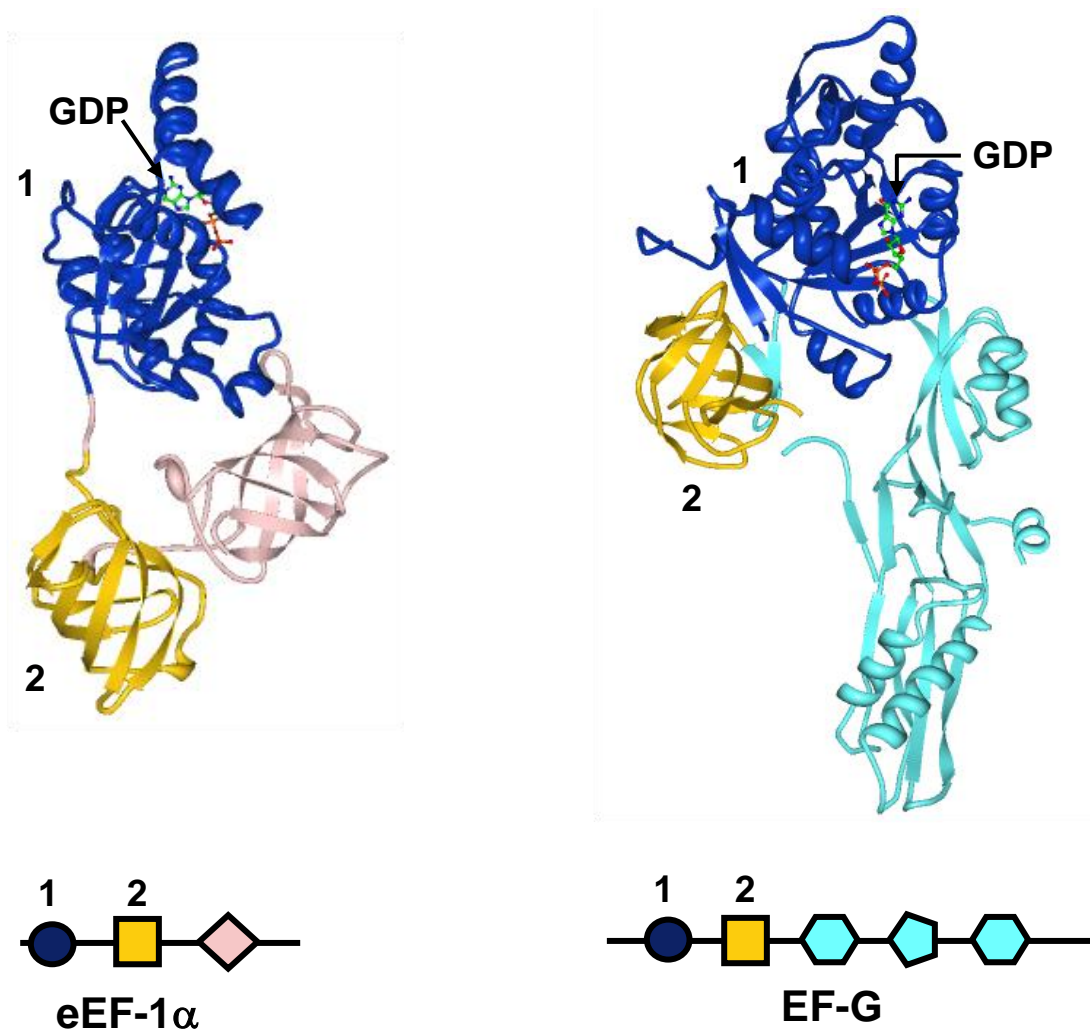


Fig. 2.2 COLOR VERSION

Modularity of protein domains, using as an example factors required for protein synthesis (elongation factor 1-alpha [eEF1- α] and elongation factor G [EF-G], both in complex with guanosine diphosphate [GDP])¹. The N-terminal domains

of both (the GDP-binding domain 1 and the 'translational protein' domain 2, as shown) are in structurally homologous families, but their C-terminal domain structure is divergent (indicated also with domain schematics below their corresponding structures, and with matched colors for homologous domains).

Sources: [Protein Data Bank](#)²; eEF1- α : [1JNY](#)³; EF-G: [1DAR](#)⁴. Images generated with Protein Workshop⁵

CHAPTER 3

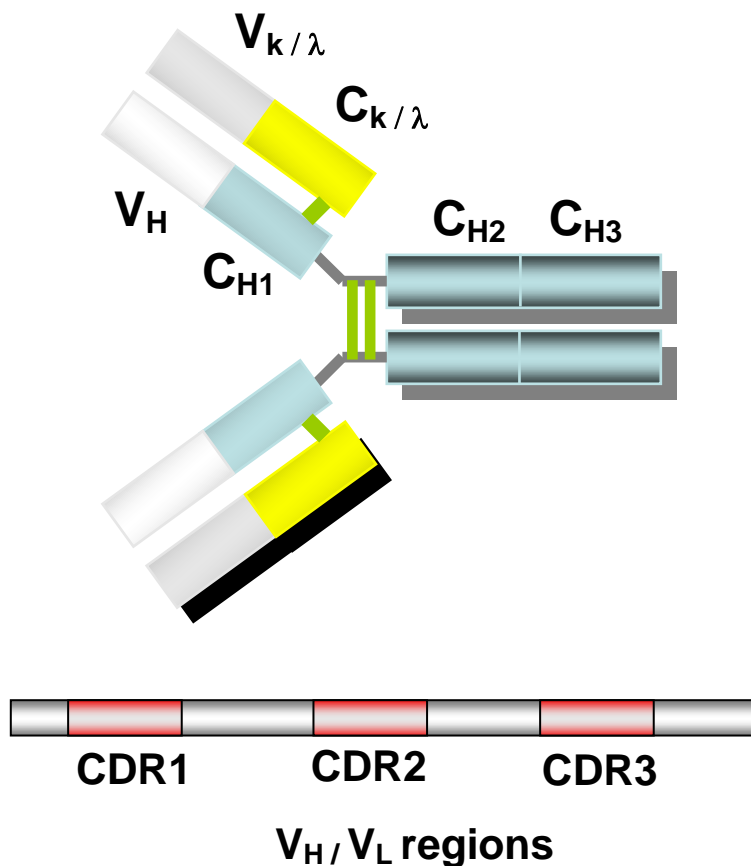


Fig. 3.1 COLOR VERSION

Schematic of general antibody (immunoglobulin) structure. V_H , heavy-chain variable region; C_{H1} - C_{H3} , constant region (domains 1-3); $V_{\kappa/\lambda}$, κ (kappa) or λ (lambda) light chain variable regions; $C_{\kappa/\lambda}$, κ or λ light chain constant regions. Chains are joined by disulfide (S-S) bonds. CDR = complementarity-determining regions for heavy and light chains. Chapter 7 (Fig. 7.1, and this site) provides more structural details for antibodies.

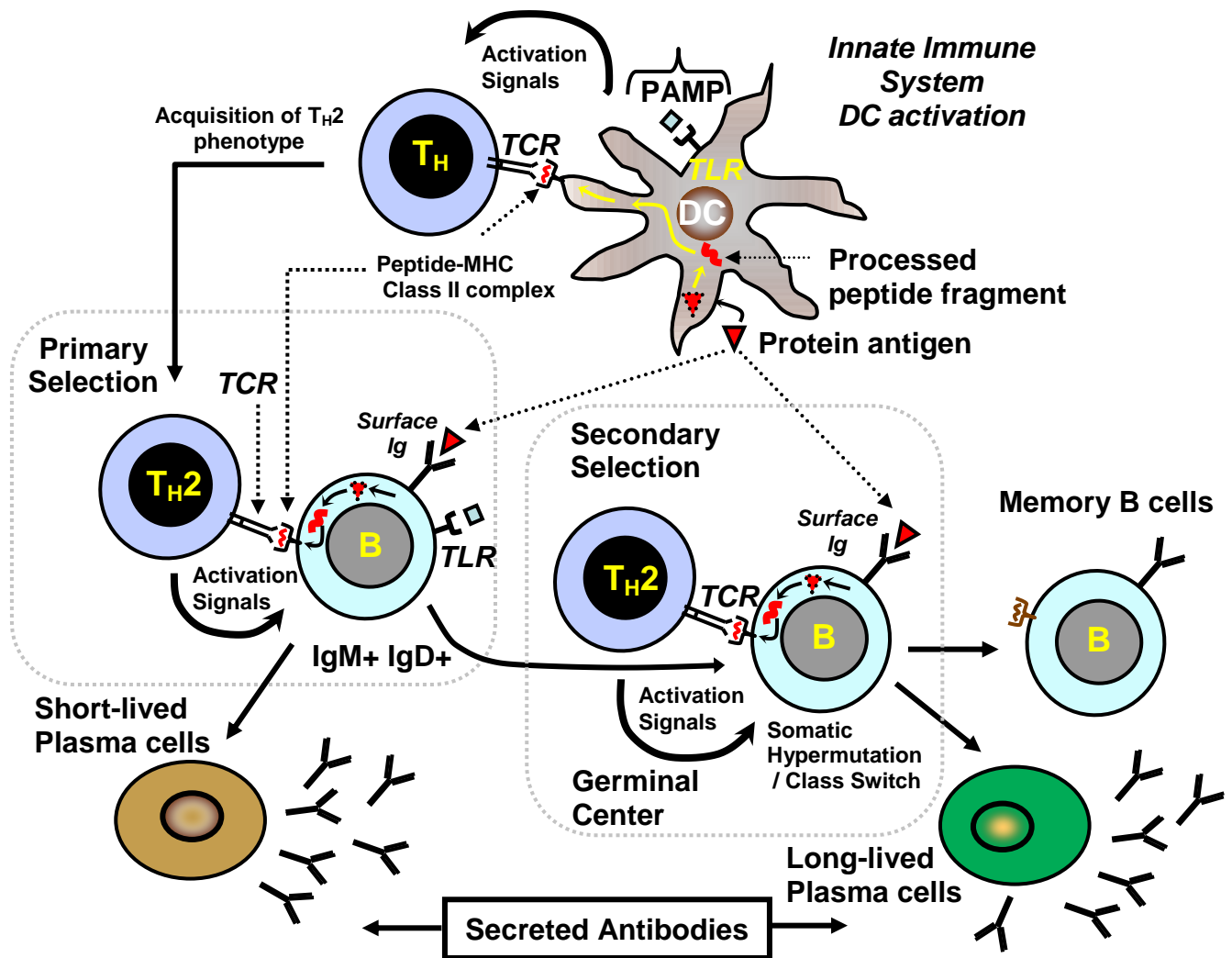


Fig. 3.2 COLOR VERSION

This is an expanded version of Fig. 3.2 of Searching for Molecular Solutions (in Chapter 3), which includes secondary selection for affinity-matured antibodies in germinal centers, and differentiation of B cells into antibody-secreting plasma cells, as shown.

Schematic showing some of the important primary interactions required for B cell activation in the adaptive immune system. Abbreviations: DC, dendritic cell; T_H,

naïve T helper cell; T_H2, T helper cell Type 2 (specific subclass of thymus-derived lymphocyte); B, B cell (bone-marrow derived lymphocyte); Ig, Immunoglobulin; PAMP, pathogen-associated molecular pattern; TCR, T cell receptor; TLR, Toll-like receptor; MHC, major histocompatibility complex protein. Innate molecular sensing can occur through either surface or intracellular recognition molecules (exemplified by TLRs here, but additional molecules also exist ⁶).

Note that this schematic has been considerably simplified in not showing many of the costimulatory signals which are essential for the differentiation events to occur. Also, interactions between dendritic cells and naïve T helper cells can also result in differentiation of different helper cell subsets, such as T_H1 cells.

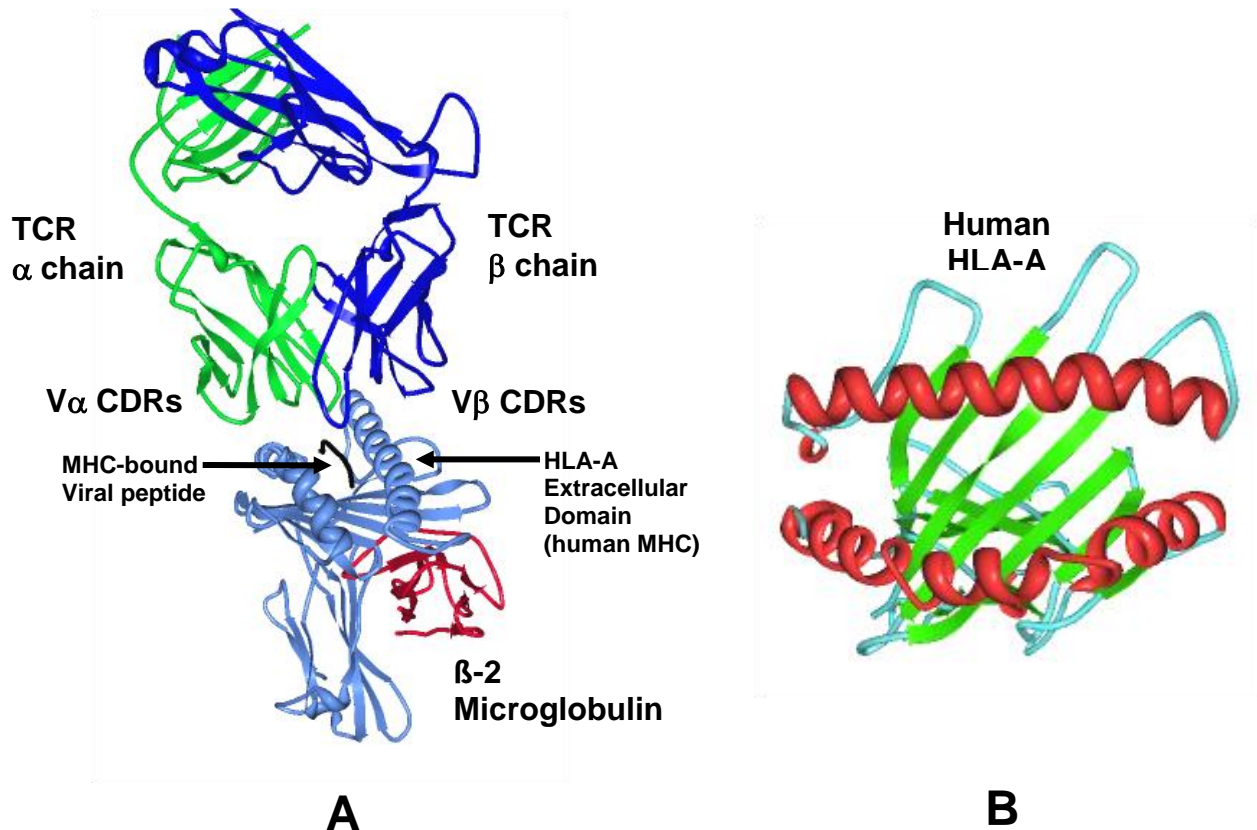


Fig. 3.4 COLOR VERSION

Structures of T cell receptor and MHC. **A.** Structure of a specific T cell receptor (TCR; α/β) complexed with Class I MHC (human HLA-A 0201) with bound viral peptide (LLFGTPVYV; tax peptide fragment from human T lymphotropic virus Type 1). β -2 microglobulin is associated with the heavy chain of HLA molecules. Only extracellular domains present; different domains shown with separate colors. **B.** Structure of Class I MHC (Human HLA-A2) heavy chain viewing the N-terminal peptide-binding groove (minus peptide) formed from a platform of antiparallel β -strands (green segments) and enclosed by α -helices (red segments). In Class I MHC, the peptide-binding groove is formed solely from the heavy chain (as in **B**); in Class II MHC it is formed from association of both the

separate α and β chains (not shown; ⁷; See Cited Notes Chapter 3 'MHC-peptide binding' in this FTP site for further information). Source: [Protein Data Bank](#) ²;
Panel A: [1BD2](#) ⁸; Panel B: [2GUO](#) ⁹. Images generated with Protein Workshop ⁵.

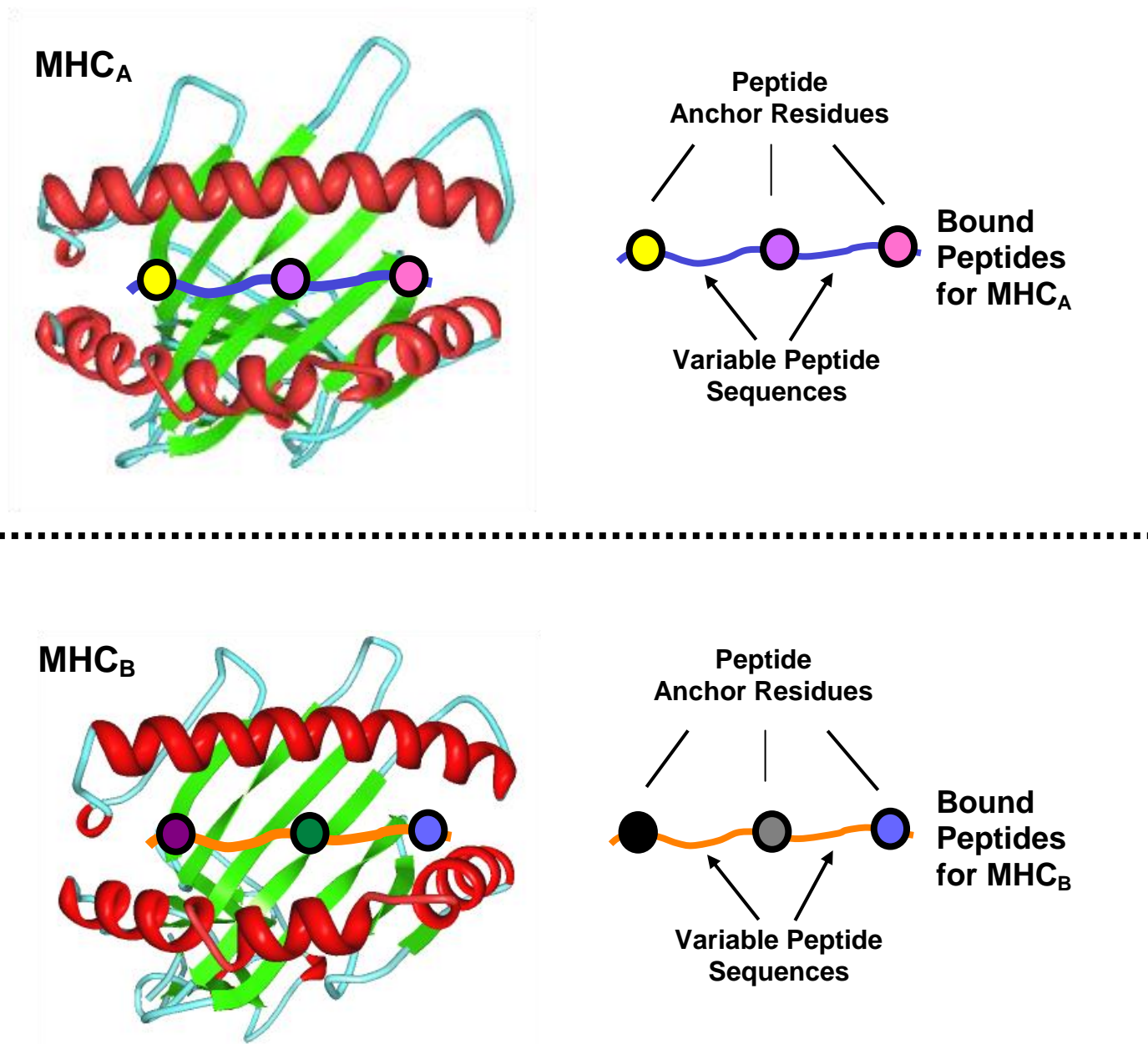


Fig. 3.5 COLOR VERSION

Depiction of MHC peptide binding. Red, green, and blue segments indicate α -helices, β -strands, and loop regions respectively. Two MHC Class I alleles (A and B, structures shown with superimposed schematic peptides in binding grooves) each can bind a large but restricted set of peptides, restricted by

defined anchor residues (colored circles). Remaining peptide residues (lines) are less constrained. Source: [Protein Data Bank](#)²; MHC_A: HLA-A2, [2GUO](#) as for Fig. 3.4; MHC_B: HLA-B*2705, [3B6S](#)¹⁰. Images generated with Protein Workshop⁵

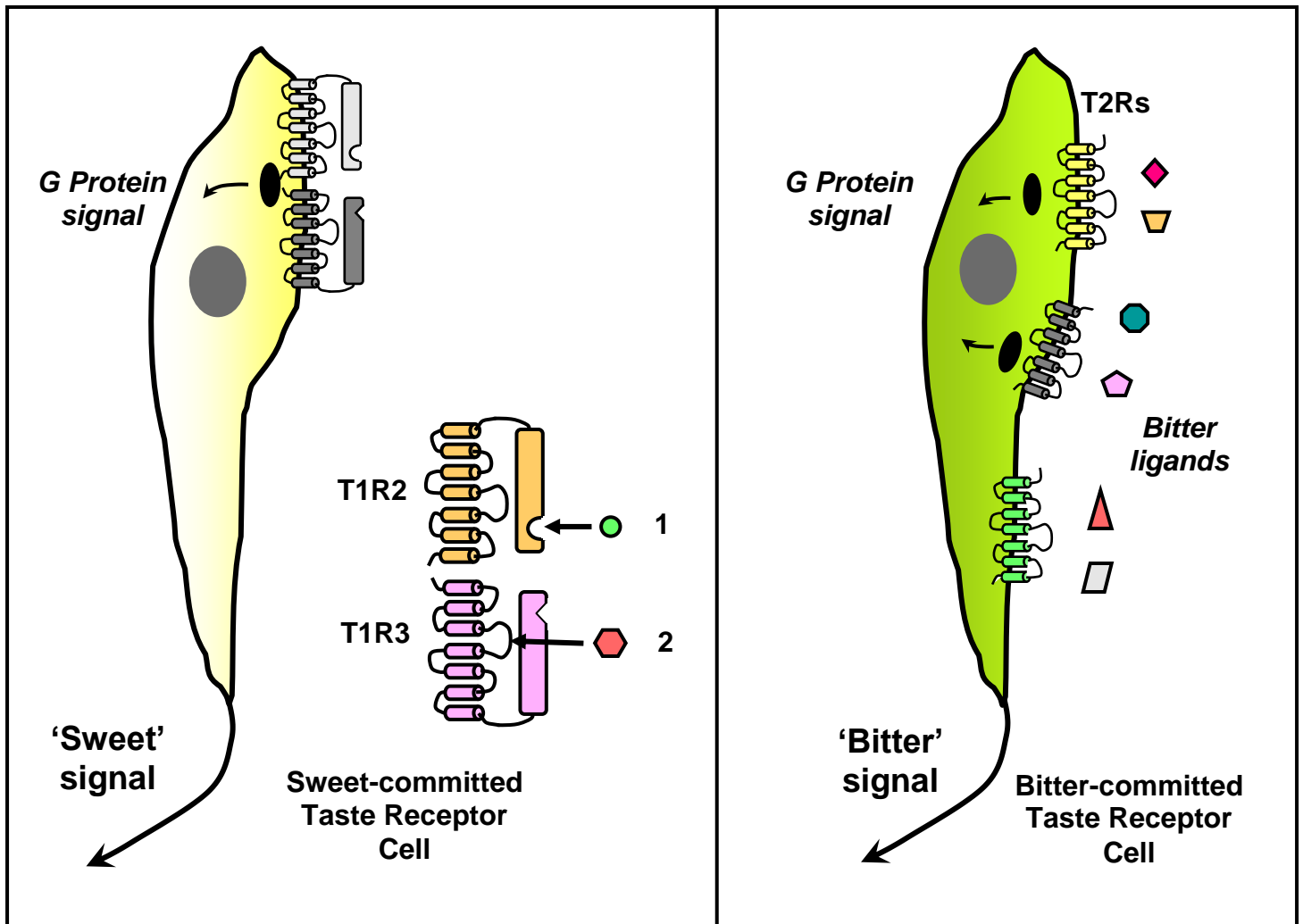


Fig. 3.7 COLOR VERSION

Schematic depictions of sweet and bitter taste receptor cells and receptors. Left panel: Sweet taste cell and receptors (T1R2 / T1R3 heterodimers of 7-transmembrane segment G Protein-coupled receptors). Ligand 1: sweet tastant N-terminal site; ligand 2: sweet tastant extracellular transmembrane site. Right panel: Bitter taste cell and receptors. T2Rs may also function as dimers; ~30 different T2Rs are believed to be expressed per cell.

CHAPTER 4

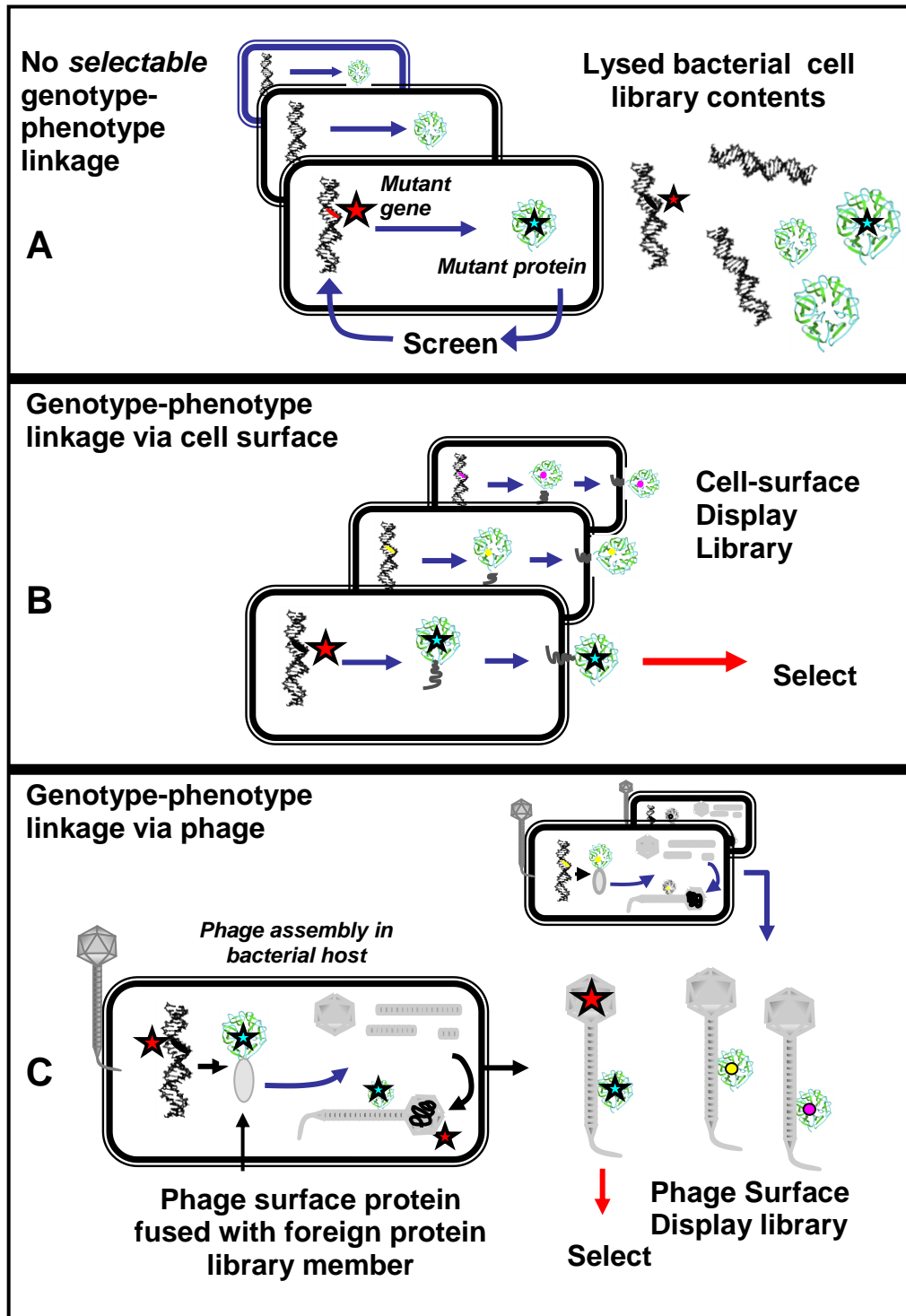


Fig. 4.9 COLOR VERSION

Depiction of certain types of genotype-phenotype linkages. Red stars indicate locations of DNA sequences encoding specific mutant library members; Blue stars indicate corresponding expressed proteins or peptides. **A**, Expression of a library of mutant proteins within bacterial cell compartments, with a single such compartment shown. Screening clones of individual cells, each with a separate mutant protein, yields the corresponding genetic information as long as clonal library members are evaluated separately. If library cells are lysed *en masse*, no linkage between mutant proteins and the gene(s) which encode them is maintained. **B**, If mutant proteins are engineered such that they are stably expressed on the surface of the bacterial cell, physical selection for a binding interaction with the surface protein also delivers the accompanying 'attached' whole cell with the appropriate genetic information. **C**, Linkage between a mutant protein and the genetic information which specifies it, via phage proteins. Phage DNA entering a bacterial host cell is engineered to encode a library of fusion proteins between the protein of interest (mutagenized as desired) and a constant phage structural gene. (All genes required for the normal phage lifecycle are left intact). Upon assembly of phage virions, the fusion protein is incorporated into the phage structure (in this example, a phage tail tube); phage DNA which includes the specific mutant protein sequence is incorporated into the phage head structure. In both B and C, selection can be based on the properties of the specific expressed surface phenotypes.

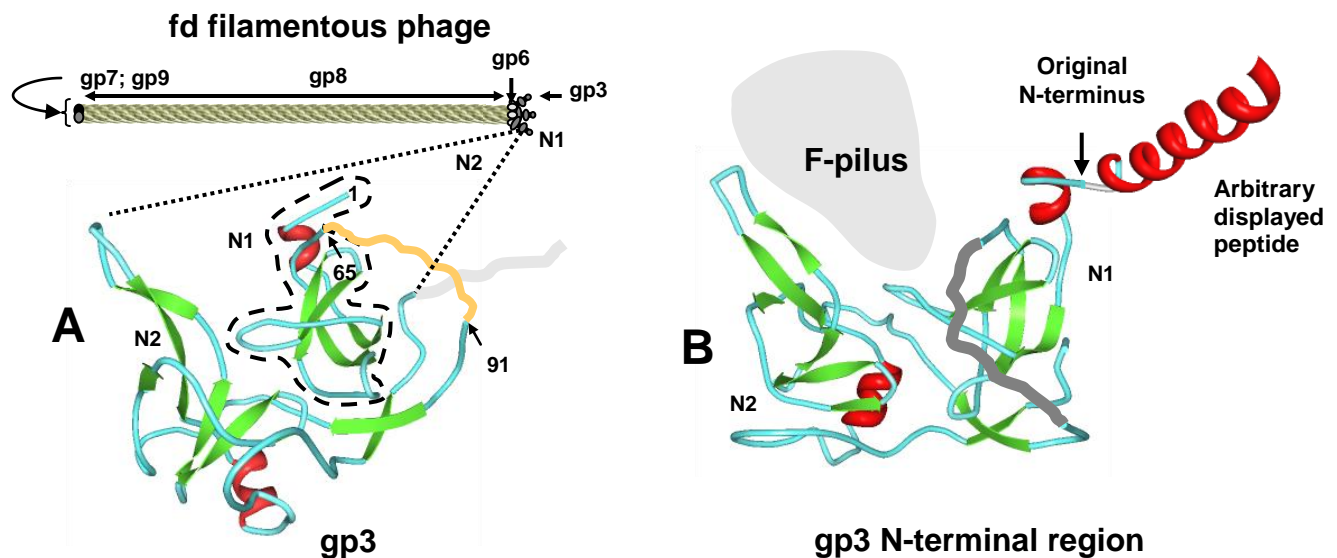


Fig. 4.10 COLOR VERSION

Structure of the filamentous phage fd (and relatives M13, f1). Red, green, and blue segments indicate α -helices, β -strands, and loop regions respectively. **A**, Phage virion showing the filament (in which the single-stranded phage genome is contained) composed of the major coat protein gp8 (product of Gene VIII), with the four minor proteins as shown at each end. The end mediating contact with the host bacterial F pilus and infection contains gp3 (product of Gene III), whose N-terminal domain structure is also shown; five copies are believed to be present in the phage filament¹¹ (N1 domain encircled with dotted line). Numbers show positions in amino acid sequence. Orange line depicts unstructured linker sequence between domains N1 and N2 (residues 65-91 as shown) also referred to as D1 and D2¹²); light gray depicts the linker region joining to the C-terminal remainder of gp3. **B**, The N-terminal region of gp3 depicting an arbitrary helical peptide sequence fused and displayed at the N-terminus. The position of the N-terminal fusion is such that it does not interfere with binding of the N2 domain to

the (schematically represented) F pilus¹³ on the bacterial host. Source of gp3 structures: [Protein Data Bank](#)²; [1G3P](#). Images generated with Protein Workshop⁵.

CHAPTER 5

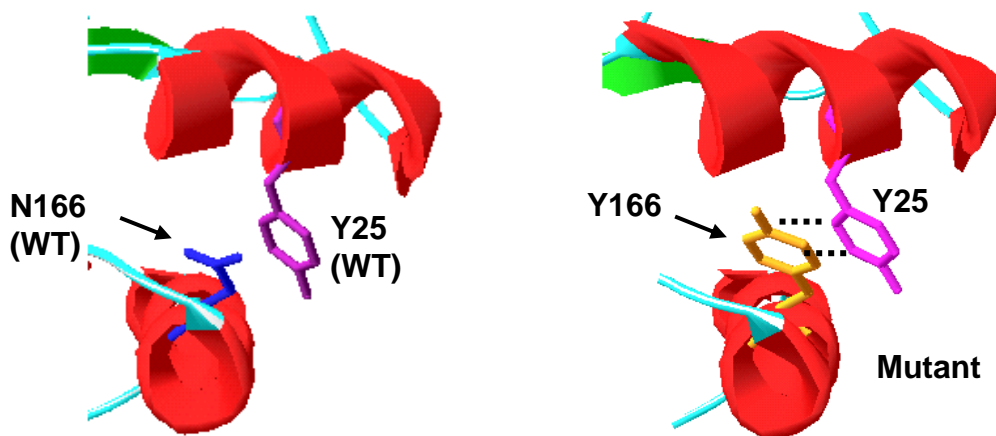
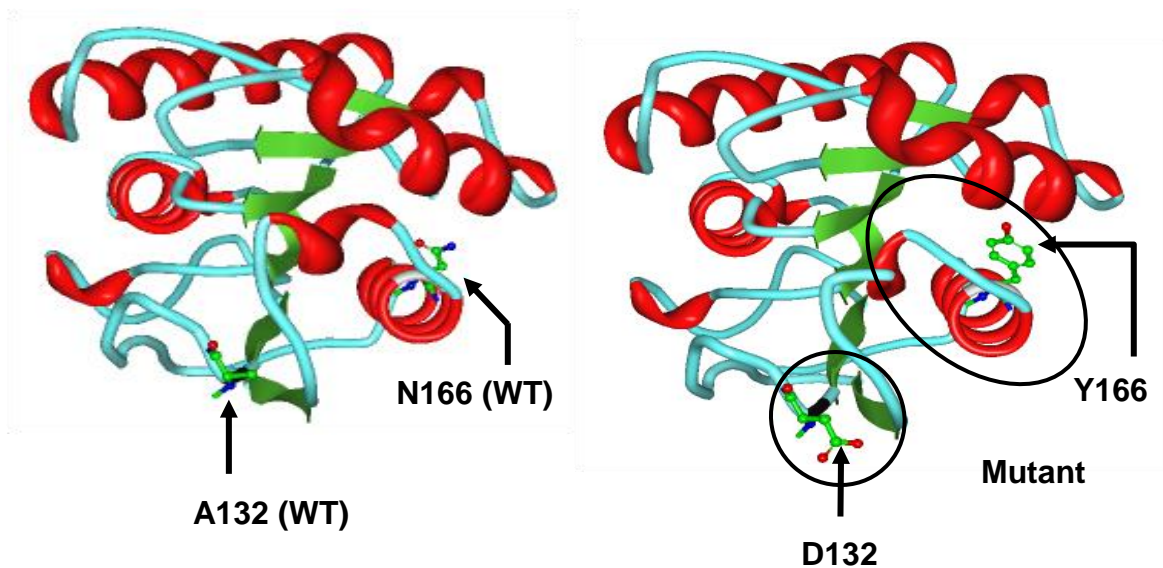


Fig. 5.1 COLOR VERSION

Structures of wild-type (WT; on left top and bottom) and mutant lipases from the bacterium *Bacillus subtilis*. Red, green, and blue segments indicate α -helices, β -strands, and loop regions respectively. **Top**, whole enzymes comparing wild-type

¹⁴ and a double mutant with 100-fold improvement in its thermal denaturation time ¹⁵, showing the side-chains for the A132D and N166Y mutation in the mutant. Sources: [Protein Data Bank](#) ²; [1I6W](#) (wild-type) and [1T4M](#) (double-mutant). Images generated with Protein Workshop ⁵. **Bottom**, regions of wild-type (left; ¹⁶) and mutant ¹⁵ lipases compared to show an example of a stabilizing interaction (aromatic base stacking between mutant tyrosine 166 [yellow] and wild-type tyrosine 25 [purple]) which enhances interhelical packing. Sources: [Protein Data Bank](#) ²; [1ISP](#) (wild-type) and [1TM4](#) (mutant). Images generated with [Swiss-pdb viewer](#) ¹⁷.

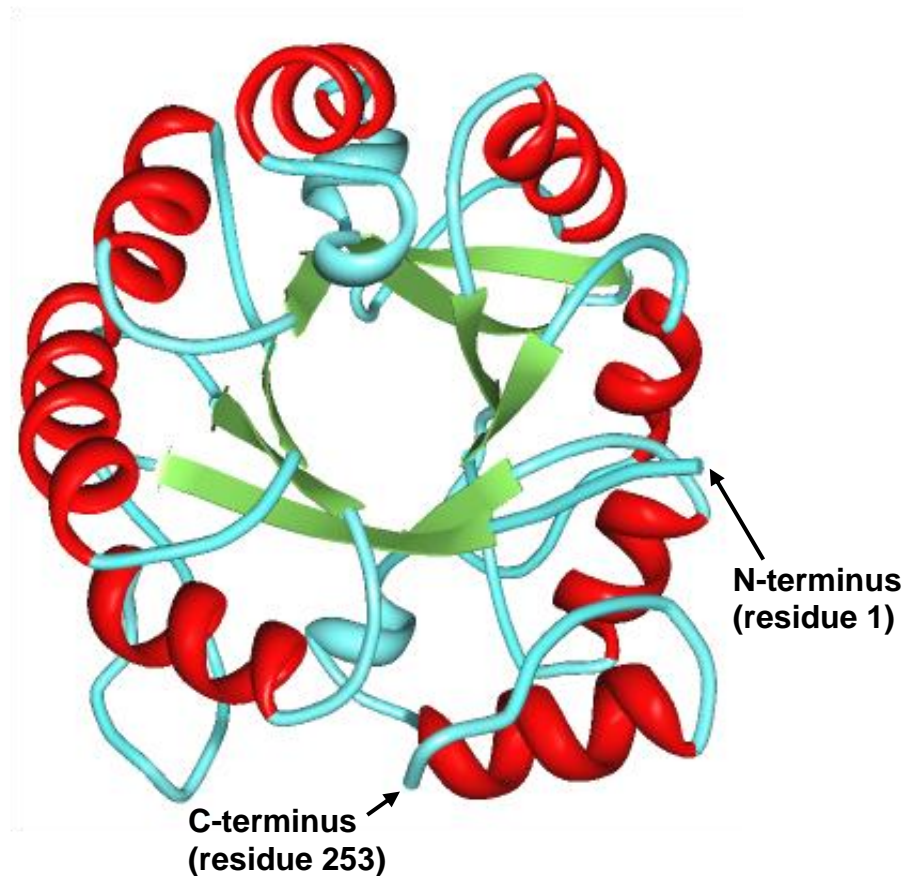


Fig. 5.2 COLOR VERSION

Structure of a representative TIM (β / α)₈ barrel scaffold protein, the cyclase subunit of imidazoleglycerolphosphate synthase (product of the *HisF* gene, a component in the histidine biosynthetic pathway) from the hyperthermophilic prokaryote *Thermotoga maritima*¹⁸. Red, green, and blue segments indicate α -helices, β -strands, and loop regions respectively. View of the β / α barrel, with N- and C-termini of protein (253 residues) is shown. (In this enzyme structural motif, the active site is always configured at the C-terminal end of the barrel's β -strands¹⁹). Source: [Protein Data Bank](#)²; [1THF](#)¹⁸. Images generated with Protein Workshop⁵.

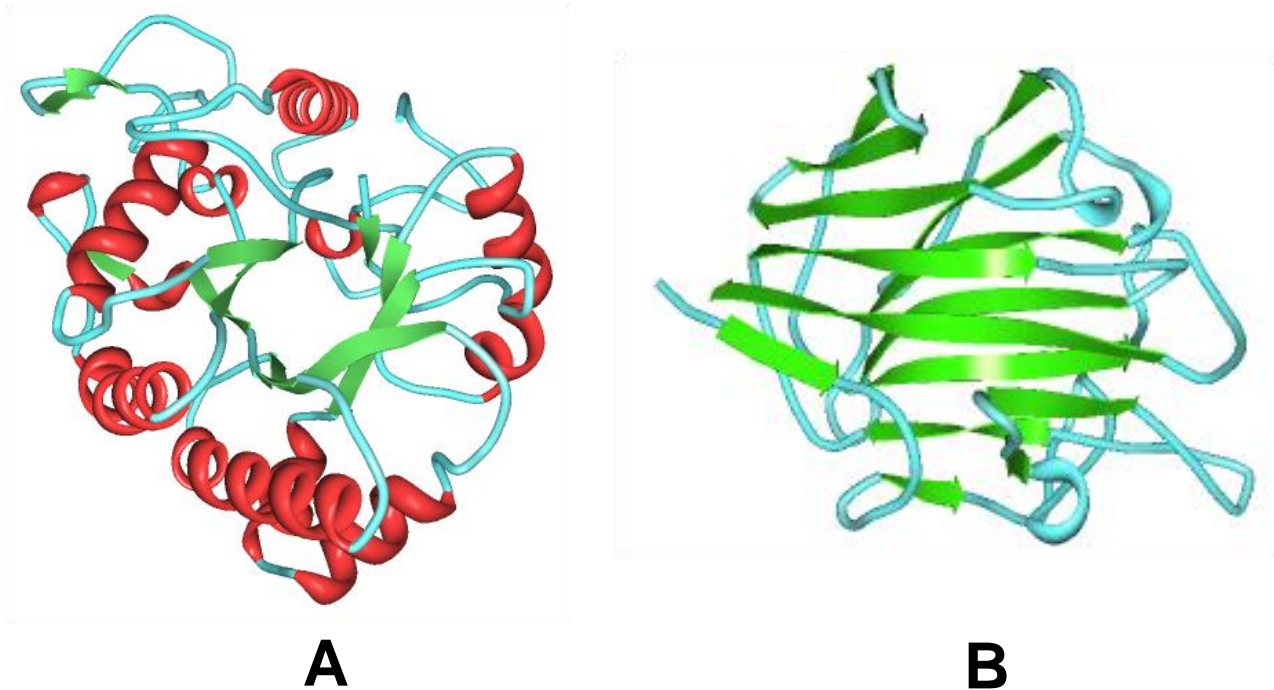


Fig. 5.3 COLOR VERSION

Examples of analogous enzymes catalyzing the same glycosyl hydrolytic reaction (both 1,3-1,4- β -D-glucan 4-glucanohydrolases; from ²⁰ and online supplement http://www.ncbi.nlm.nih.gov/Complete_Genomes/AnalEnzymes.html). Red, green, and blue segments indicate α -helices, β -strands, and loop regions respectively. **A**, Enzyme from barley with a TIM barrel fold ²¹; **B**, Enzyme from *Bacillus macerans* (showing one subunit of a homodimer), with a very different fold ('sandwich jellyroll'; Concanavlin A-like lectin fold), almost all β -strand ²². Source: [Protein Data Bank](#) ²; A, [1GHR](#); B, [1MAC](#). Images generated with Protein Workshop ⁵.

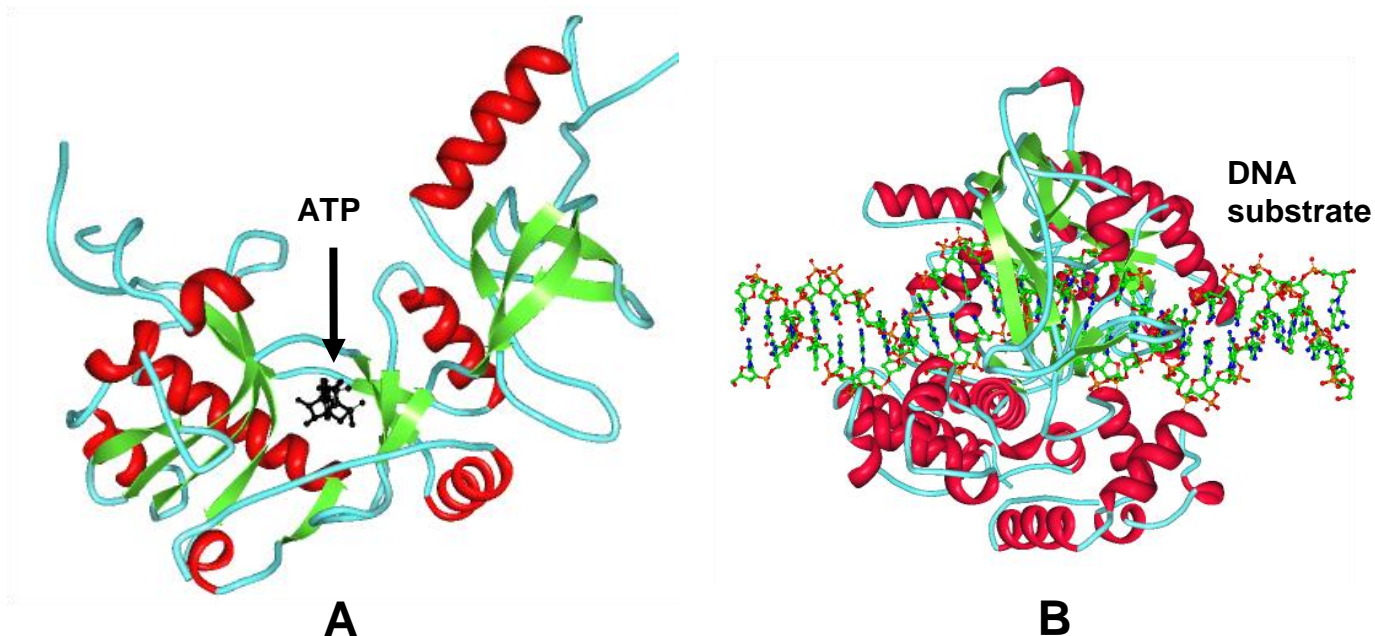


Fig. 5.4 COLOR VERSION

Structures of DNA ligases. Red, green, and blue segments indicate α -helices, β -strands, and loop regions respectively. **A**, DNA ligase from *E. coli* bacteriophage T7²³ showing substrate binding cleft with cofactor ATP within it; **B**, *E. coli* DNA ligase with a (nicked) DNA substrate enveloped within a 'protein clamp'. Source: [Protein Data Bank](#)²; A, [1A0I](#); B, [2OWO](#). Images generated with Protein Workshop⁵.

MODIFIED BASES

G: 2-methylguanosine; **U:** 5,6-dihydrouridine; **G:** N²-dimethylguanosine; **C:** O²-methylcytidine;
G: O²-methylguanosine; **W:** wybutosine; **U:** pseudouridine; **C:** 5-methylcytidine; **G:** 7-methyl-
 guanosine; **U:** 5-methyluridine; **A:** 1-methyladenosine

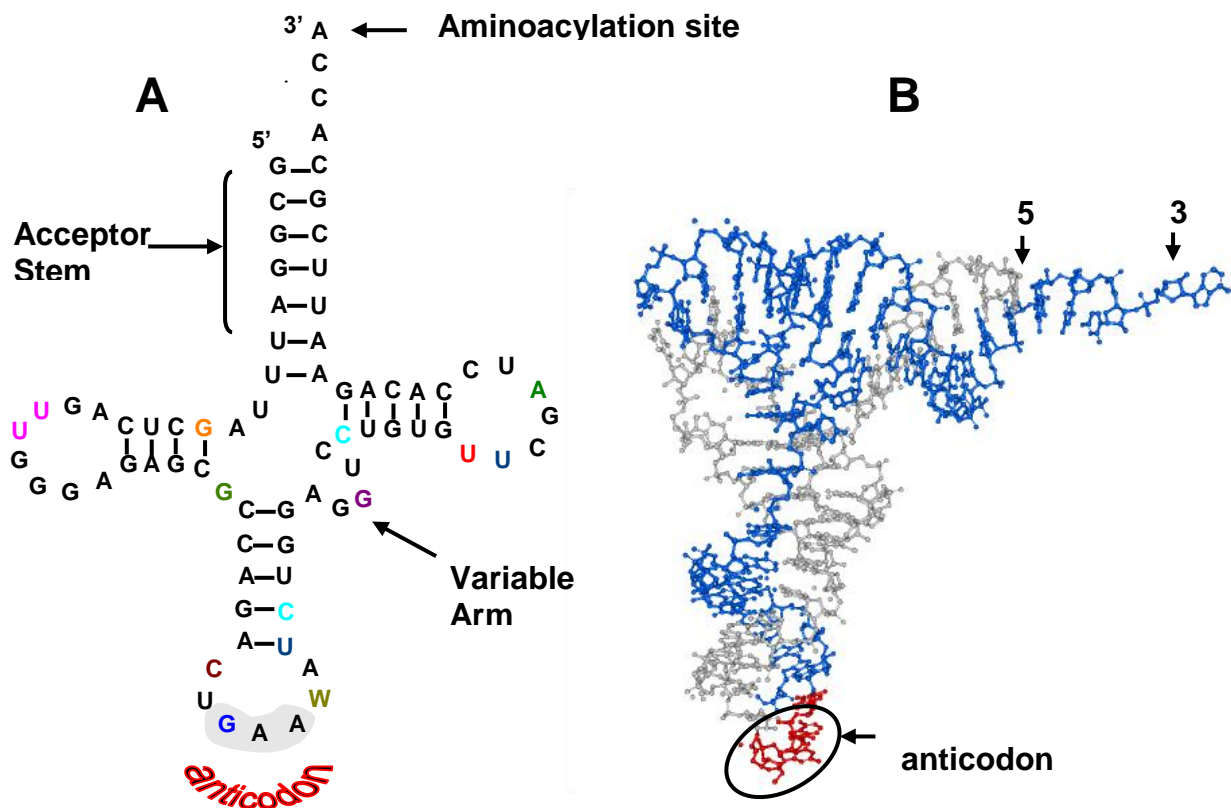


Fig. 5.6 COLOR VERSION

tRNA structural arrangements with example of 76-base yeast phenylalanine-tRNA. **A**, Classic 'cloverleaf' diagram of this tRNA secondary structure, showing conventional hydrogen bonding (lines), enzymatically-modified unusual bases, and GAA anticodon. Note that the third 'wobble' position G in the anticodon (with respect to the UUC codon) is itself a modified guanosine residue. **B**, Tertiary (crystal) structure of this same tRNA. Bases 1-33 shown in gray, 34-36 (anticodon, red; circled) and 37-76 in blue. Source: [Protein Data Bank](#)²; [1EHZ](#)²⁴. Images generated with Protein Workshop⁵.

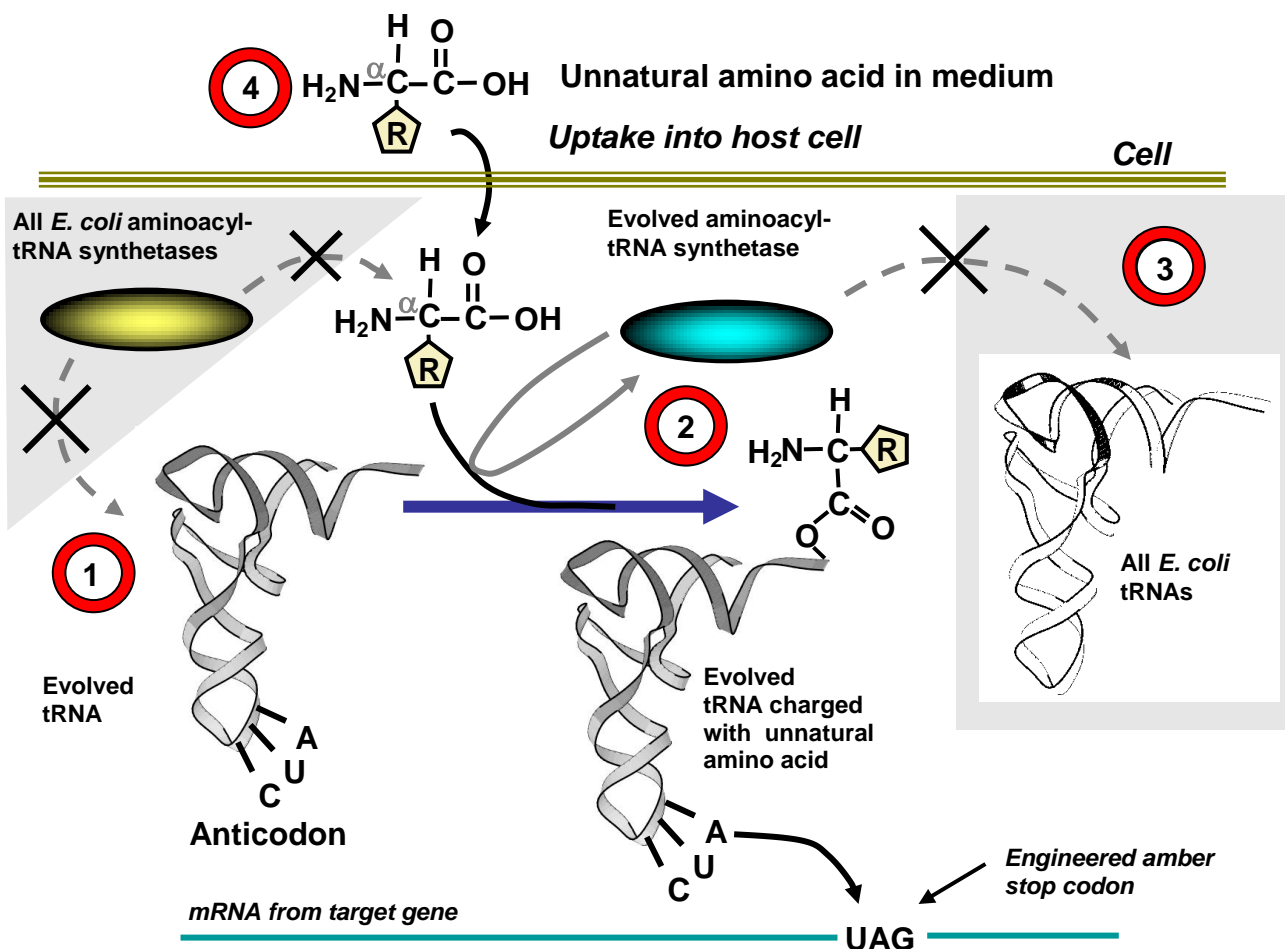
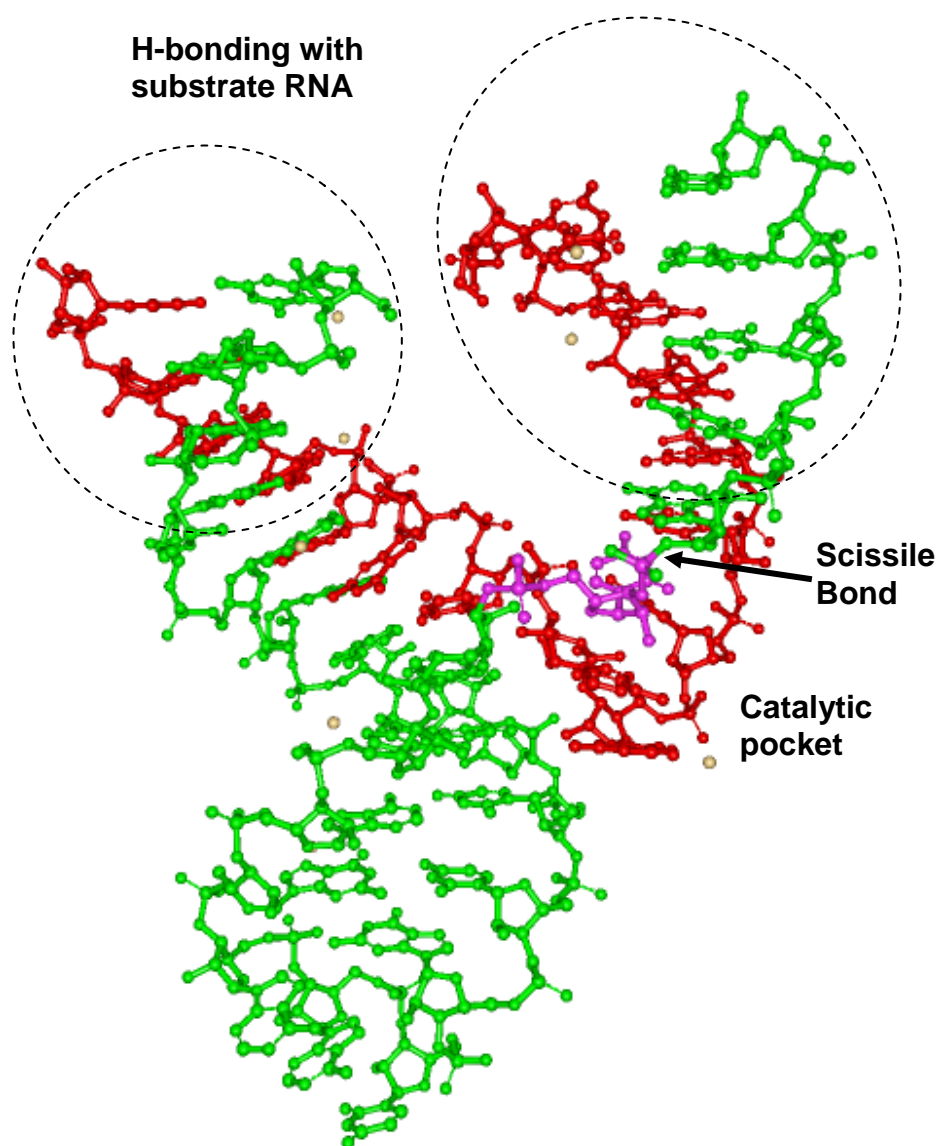


Fig. 5.10 COLOR VERSION

Requirements for expanded genetic code *in vivo* (in *E. coli* in this example) with ‘orthogonal’ tRNA and aminoacyl-tRNA synthetases^{25,26}. (1), A tRNA with an appropriate anticodon for suppression of a target stop codon (amber UAG in this example) must be altered (by directed evolution) such that it is functional in *E. coli* but not charged by any host cell aminoacyl-tRNA synthetases. Also, the latter host enzymes must not charge any *E. coli* tRNAs with the desired unnatural amino acid. (2), An aminoacyl-tRNA synthetase must be obtained (again by targeted mutagenesis and directed evolution) which charges its orthogonal tRNA with a desired unnatural amino acid (and no other natural amino acid), but at the

same time (3) fails to charge any host cell tRNA. (4) The unnatural amino acid must be transportable into the host cell. (An alternative available in some cases is to transfer exogenous biosynthetic machinery such that the unnatural amino acid can be synthesized in the host cell from common precursor molecules.

CHAPTER 6



[Fig. 6.1](#) COLOR VERSION

Structure of a hammerhead ribozyme (red) in complex with RNA substrate (green) ²⁷. The C residue 5' to the scissile bond site shown in purple (bond indicated with arrow). Regions of conventional H-bonding which direct the ribozyme to the target sequence specificity are indicated, as is the ribozyme

catalytic pocket which contains invariant base residues. (The catalytic pocket is essential for activity, but the H-bonding regions can be arbitrarily altered for designed complementarity with a substrate bearing a GUC triplet). Source:

[Protein Data Bank](#)² ; [488D](#). Images generated with Protein Workshop⁵

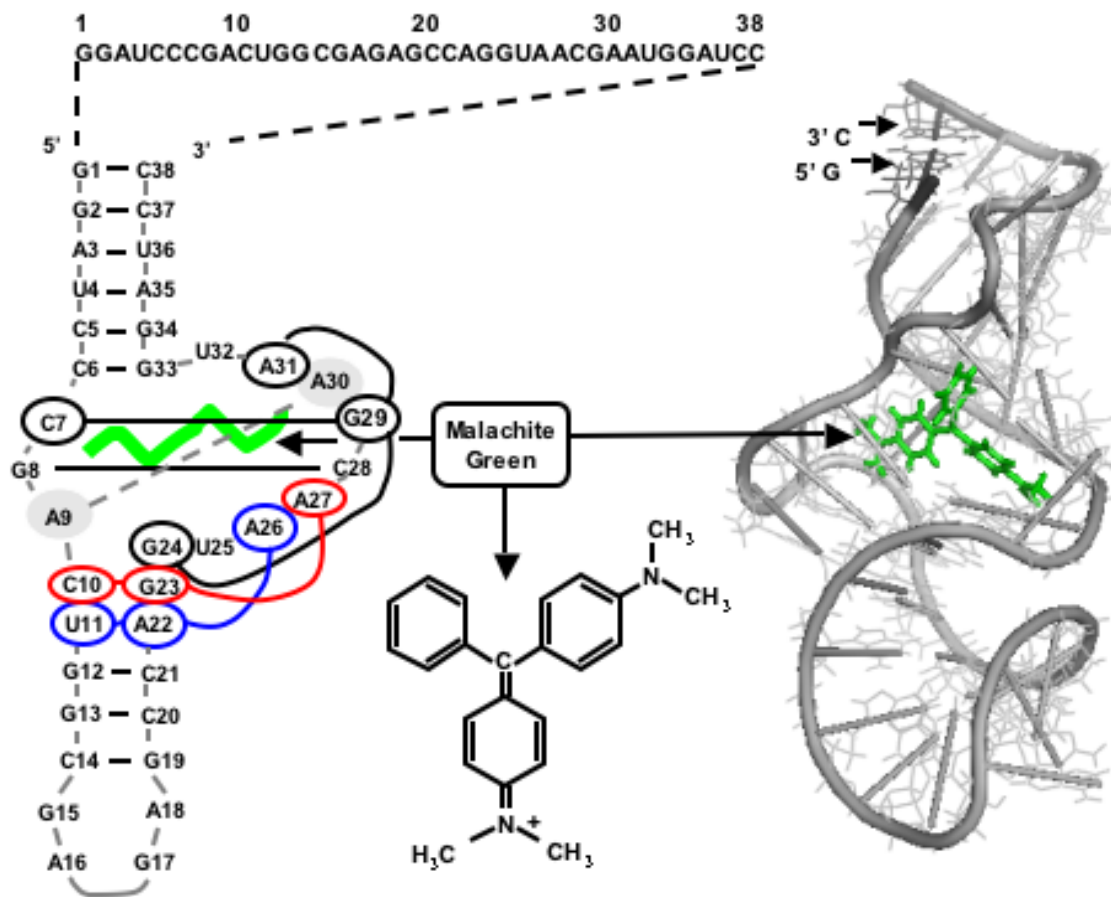


Fig. 6.7 COLOR VERSION

Sequence and solution structure of an aptamer binding the dye Malachite Green (structural formula of dye as shown). The primary RNA sequence is shown with a schematic of the secondary structure on the left, and representation of the tertiary solution structure of the aptamer complexed with Malachite Green on the right²⁸. In the schematic, normal (canonical) Watson-Crick bonds shown by horizontal black lines, base triplexes (A26 U11:A22) and (A27 C10:G23) by blue lines / circles and red lines / circles respectively; and quadruple interactions (G24 A31 G29:C7) by black lines / circles as shown. A9 and A30 (stacking interaction)

shown with gray circles. For tertiary structure, phosphodiester backbone shown (dark gray) with bases light gray; 5' and 3' positions as marked. Position of bound Malachite Green (green) as indicated. Source: [Protein Data Bank](#)²; [1Q8N](#).

Tertiary structural image generated with PyMol ([DeLano Scientific LLC](#)).

CHAPTER 7

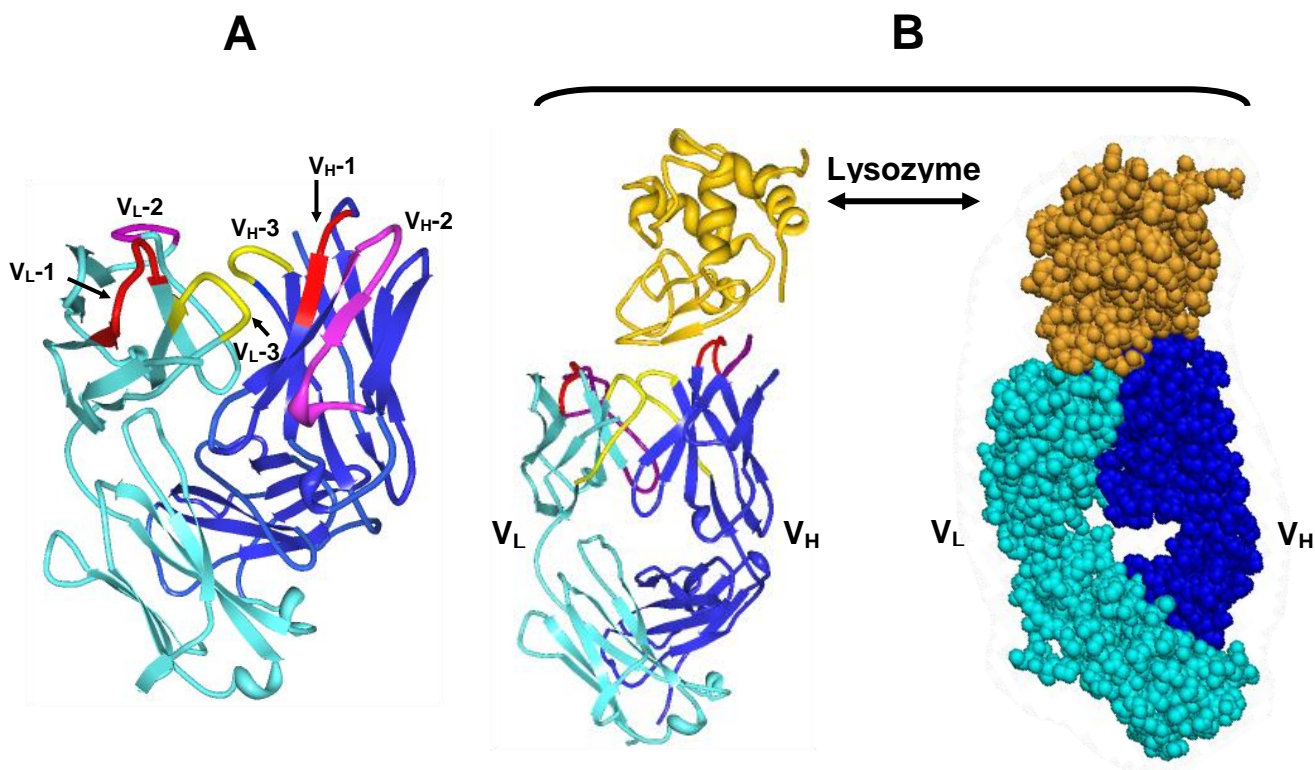


Fig. 7.1 COLOR VERSION

Structures of antibodies, represented by Fab fragments (monovalent antigen-binding fragments of whole immunoglobulins; see Fig. 7.2 of *Searching for Molecular Solutions*) from a monoclonal antibody (D44.1) against hen egg lysozyme²⁹. **A**, Isolated Fab fragment light chains (light blue) and heavy chains (dark blue), with the complementarity-determining regions (CDRs) as shown (V_H-1 = heavy chain CDR1, etc; CDRs1-3 colored red, purple, and yellow respectively). **B**; Same antibody Fab fragment complexed with its antigen lysozyme (same color scheme for heavy and light chains; lysozyme orange), On left, ribbon backbone image, on right, space-filling view. Source: [Protein Data](#)

[Bank](#)²; [1MLB](#) (left panel); [1MLC](#) (right panel). Images generated with Protein Workshop⁵. (ribbon diagrams) and PyMol (space filling; DeLano Scientific).

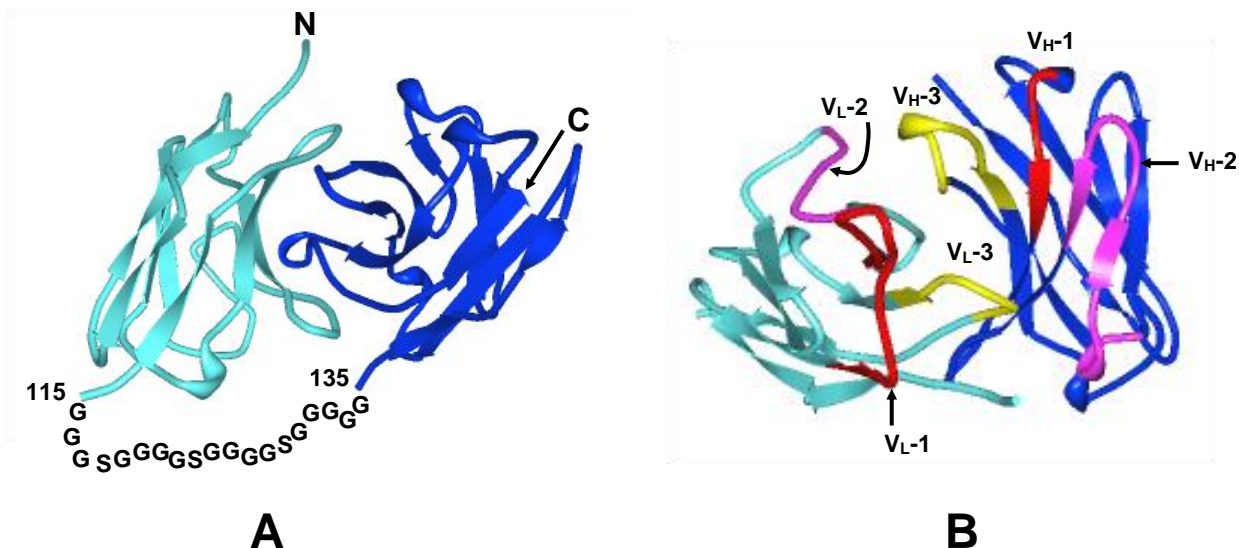


Fig. 7.3 COLOR VERSION

Structure of a specific single chain-Fv construct³⁰. **A**, The light chain variable region segment (light blue, N-terminus (N) as shown) ends at residue 115 and is linked to the N-terminus of the heavy chain (dark blue) segment at position 135 via a serine-glycine linker G₃(SGGGG)₄G as depicted (as an unstructured segment, the linker is not directly visible in X-ray diffraction images). The position of the C-terminus of the whole structure is as shown (C). **B**, The same structure looking down the antigen-binding region, with CDRs for light and heavy chains as shown (red, purple and yellow for CDRs1-3, respectively). Source: [Protein Data Bank](#)²; [2GJJ](#). Images generated with Protein Workshop⁵ with serine-glycine linker superimposed in the left panel.

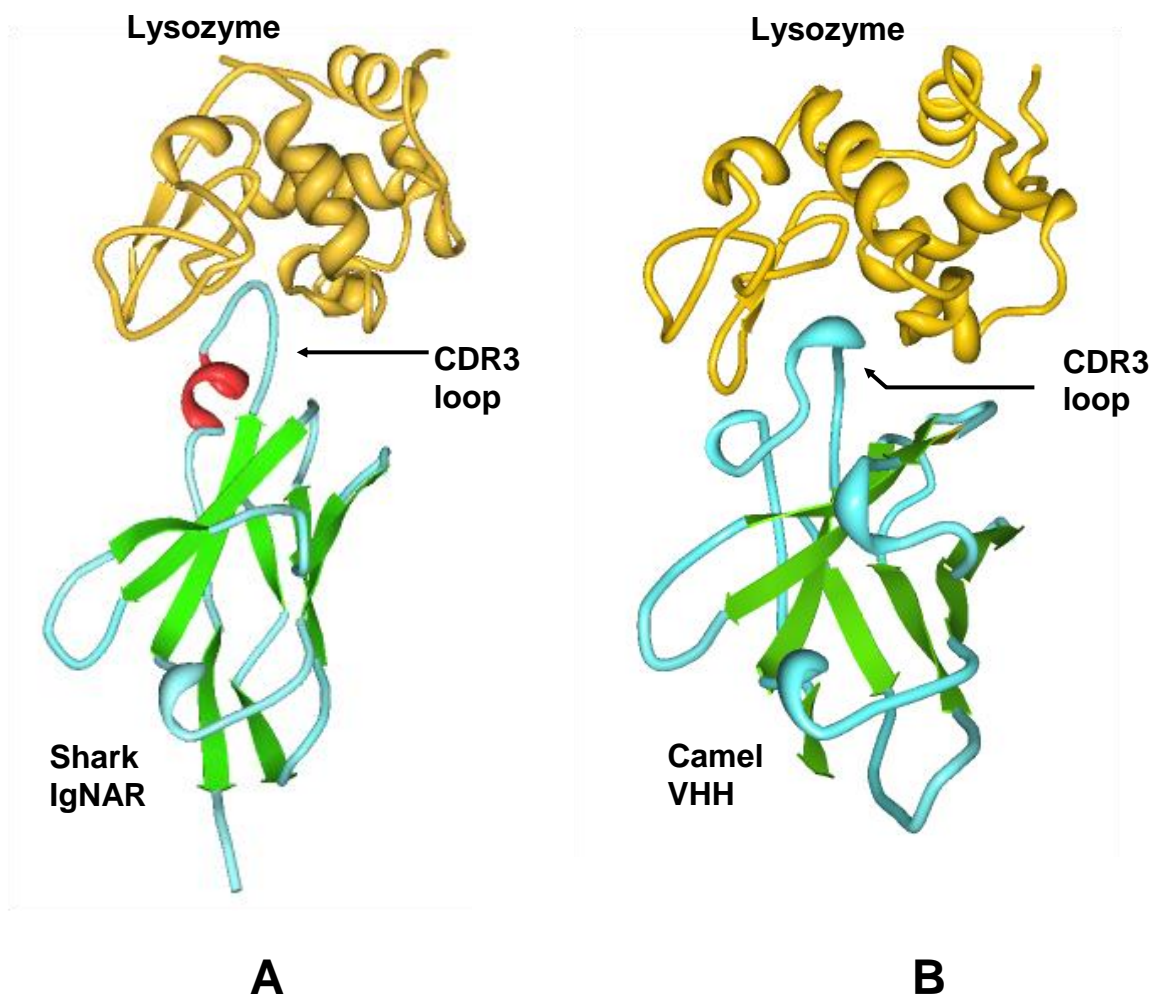


Fig. 7.5 COLOR VERSION

Comparison of crystal structures of the antigen recognition domains of shark IgNAR³¹ (A) and camel (dromedary) VHH molecules³² (B). α -helices red; β -strands green; remainder (including variable loops) light blue, both complexed with a common target antigen, lysozyme (orange). Source: [Protein Data Bank](#)² Shark IgNAR: [2I25](#); Camel VHH: [1ZVY](#). Images generated with Protein Workshop⁵.

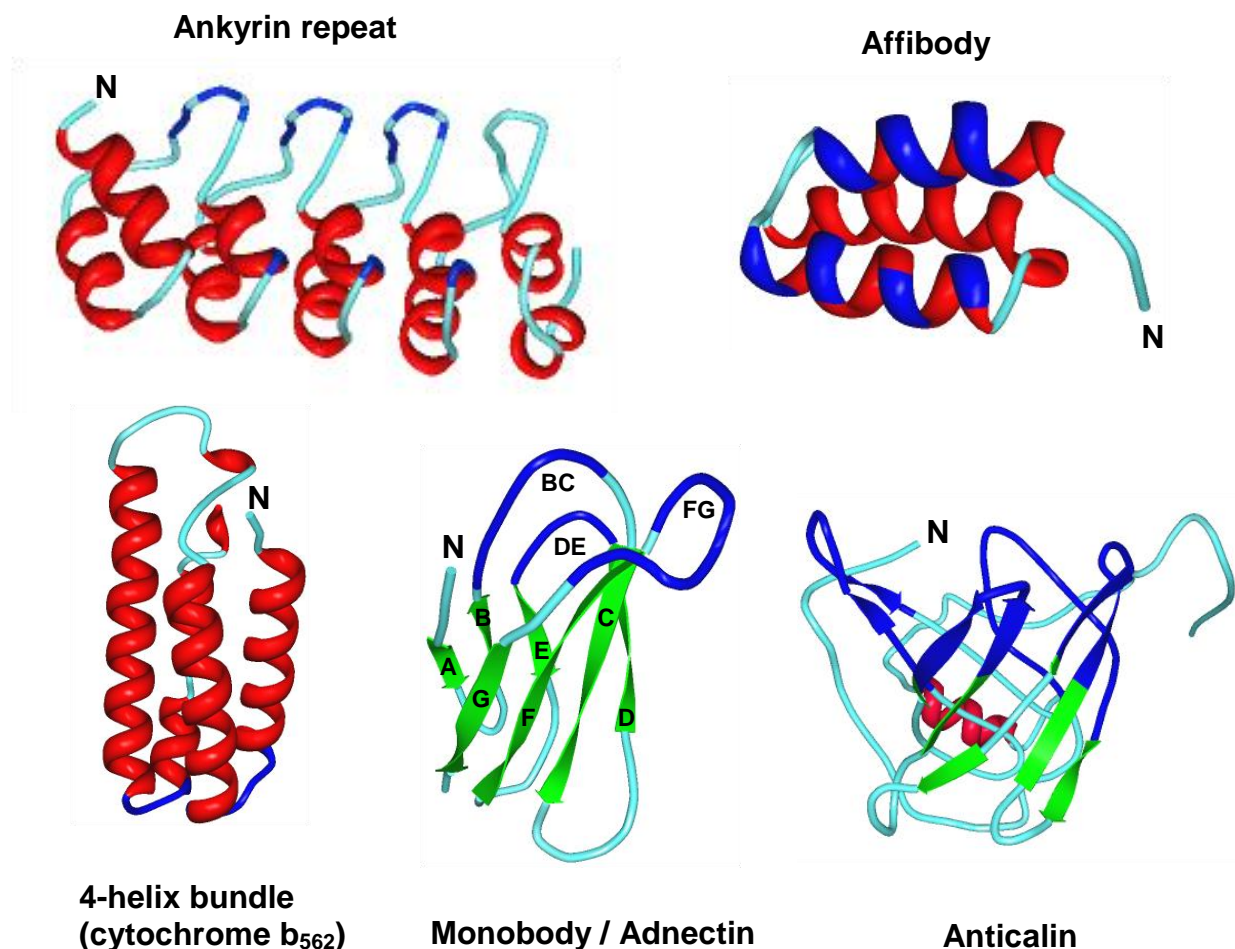


Fig. 7.9 COLOR VERSION

Structures of some alternative scaffolds for molecular recognition. Turns and coils light blue, β -strands green, α -helices red; randomized regions in dark blue. N = N-termini. Sources: [Protein Data Bank](#)²: Ankyrin repeat³³ ([1SVX](#)); affibody³⁴ ([1H0T](#)); four-helix bundle cytochrome b₅₆₂ structure³⁵ ([1M6T](#))³⁶; Monobody / adnectin ([1FNA](#))³⁷, β -strands A-G and loops shown (compare with schematic of Fig. 7.8 in *Searching for Molecular Solutions*), randomized loops as for³⁸; anticalin ([1TOV](#))^{39,40}. Images generated with Protein Workshop⁵.

CHAPTER 8

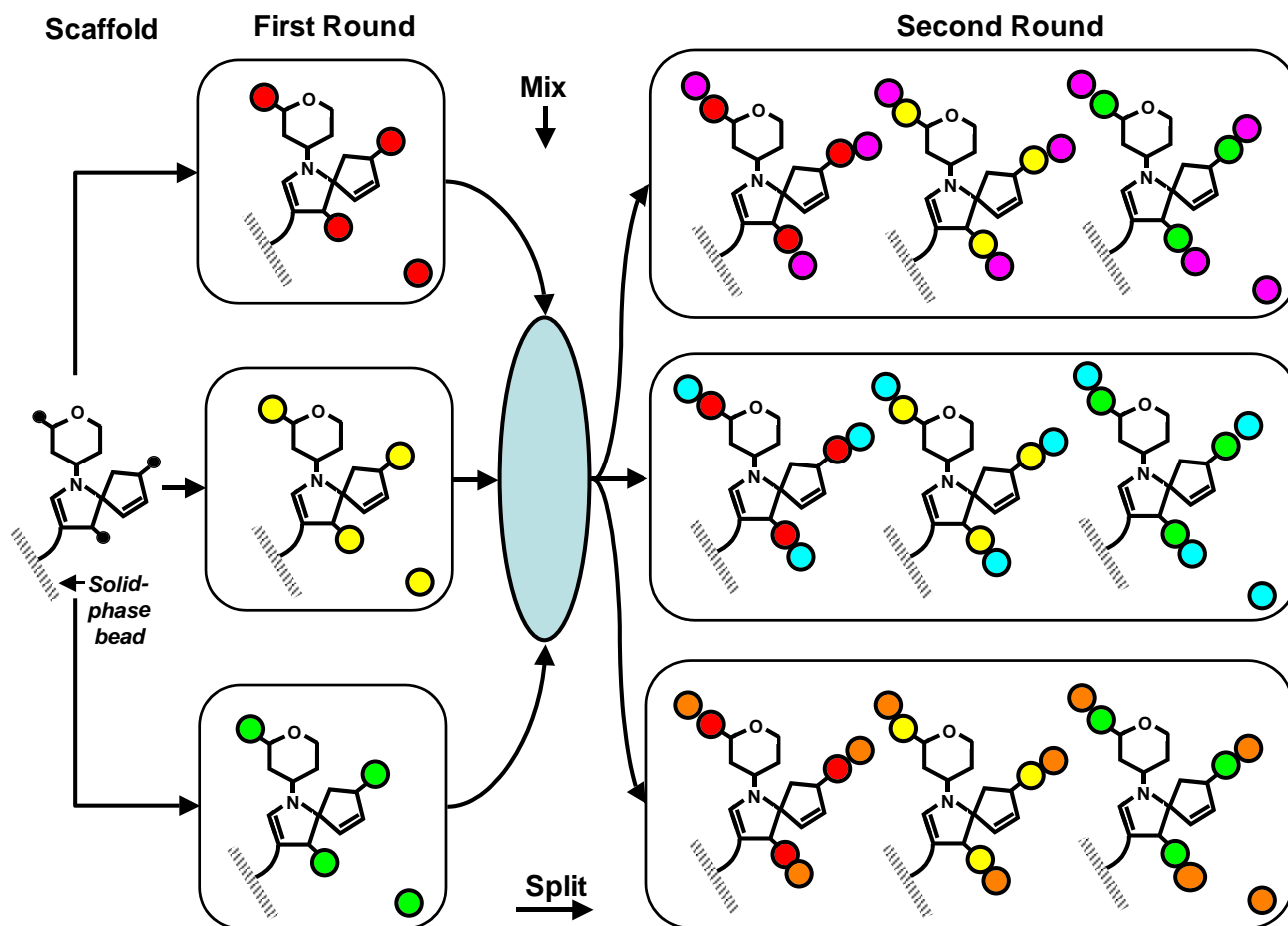


Fig. 8.5 COLOR VERSION

'Mix and split' approach to combinatorial library generation from a starting framework scaffold structure on solid-phase beads. A small library can be produced after even the first round of derivatization, and successively diversified in succeeding rounds. Synthesis begins on a pre-determined structural scaffold with a limited number of reactive groups (black dots). In any one round, each separate compartment undergoes reaction with a specific chemical reagent (dots in right-hand corner of each capsule in the diagram) to produce a derivative

which is capable of further reactivity. After a reaction round, mixing the products and redistributing them into new reaction compartments allows progressive diversification as indicated. (The process can be repeated beyond the second round as many times as desired). Note that each reaction solid-phase bead carries a unique chemical species; identification of functionally-selected compounds requires a means for encoding the synthetic combinatorial information and a means for reading it out after selection.

CHAPTER 9

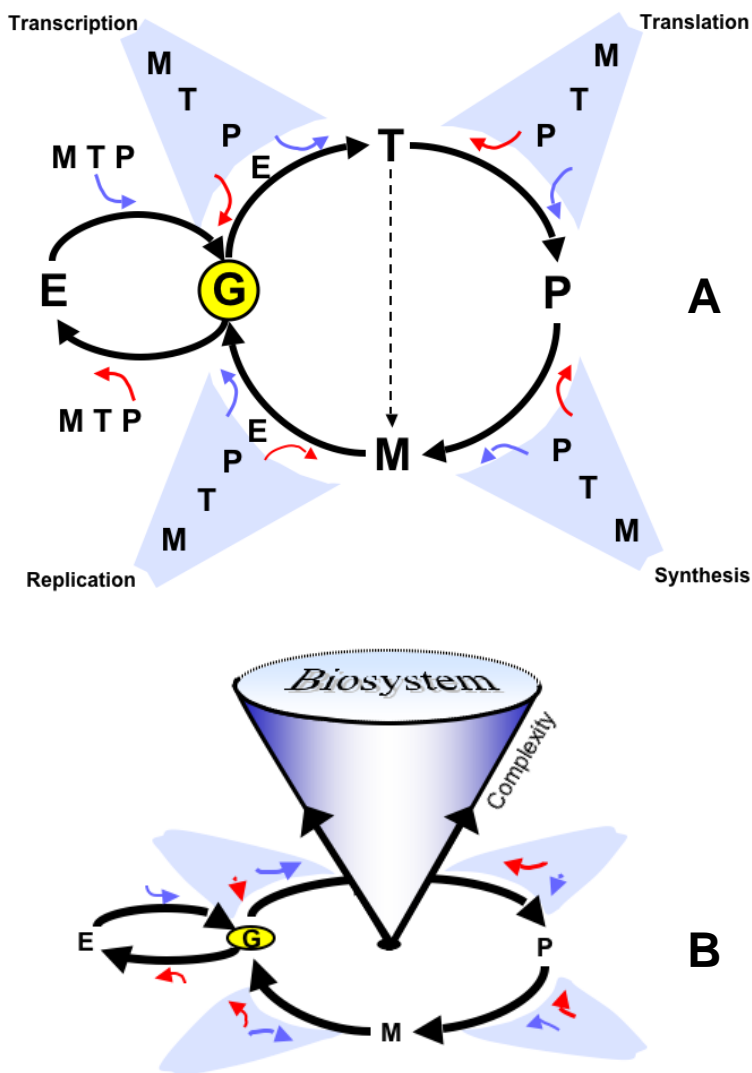


Fig. 9.7 COLOR VERSION

A. 'Omic' relationships as a cycle. Code: **G** = Genome, **T** = Transcriptome, **P** = Proteome, **M** = Metabolome, **E** = Epigenome. In this cycle, the genome gives rise to the transcriptome, and a portion of the latter in turn gives rise to the proteome. (For simplicity, in the case of eukaryotes, mitochondrial and other

organelle genomes are subsumed into the general 'Genome' category, though of course they are replicatively distinct). A portion of the proteome is concerned with synthesizing and processing small molecules (the metabolome), which are required for a variety of purposes at various points of this cycle. The metabolome (M) is shown as directly cycling back to the genome because specific parts of the metabolome (dNTPs; synthesized via the proteome) are required for DNA synthesis and physically become incorporated into replicated genomes. Each of these steps requires the feeding back and participation of specific members of the proteome, the transcriptome, and the metabolome for completion, which proceeds in a forward positive direction (small blue arrows; clockwise) or is controlled and regulated (negative direction; anti-clockwise small red arrows). The epigenome is derived from the genome by chemical modification (especially methylation), and serves as an additional regulator of transcription and genomic replication itself. The dotted line from the transcriptome to the metabolome indicates the former pathway during the RNA World. Note that in a specific organism, not all small molecules required for life processes are synthesized, since many can be acquired from the environment, but all organisms produce a fraction of their required small molecules through their own agency. See Cited Notes file; Chapter 9 in the ftp site for further details. **B.** The same diagram used to represent the great 3-dimensional and temporal complexity of biosystems arising from the 1-dimensional genomic information string.

Note that the 'ON' (or 'forward) state for the epigenome in this diagram is essentially negative regulation (adding epigenetic tags such as 5-methylcytosines usually acts to block gene expression; reversible by removing the tags enzymatically). Further information relevant to this scheme is provided in this ftp site; see Cited Notes for Chapter 9, Section 30.

CHAPTER 10

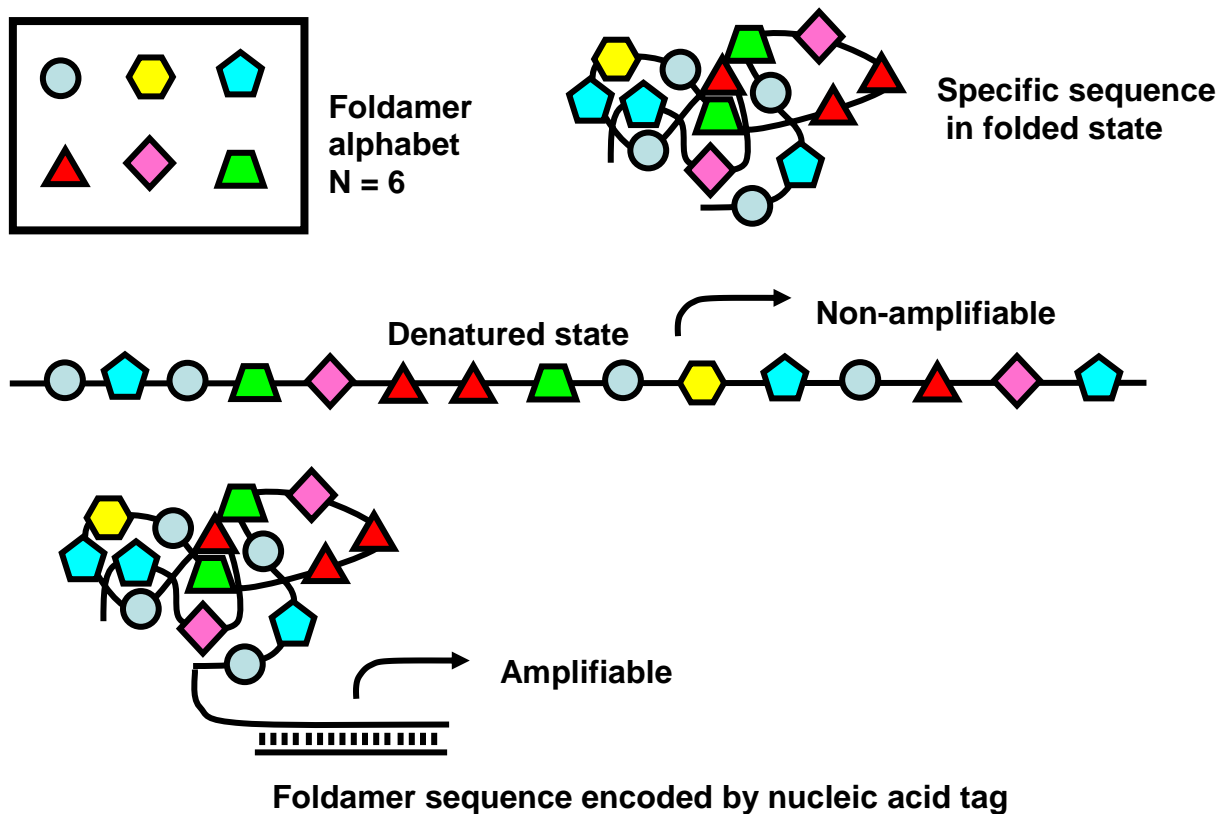


Fig. 10.2 COLOR VERSION

Depiction of a non-biological foldamer with an alphabet of six polymerizable side chain groups. From a random chemically-generated library of length 15 residues, a specific sequence (as shown) is functionally selected, but cannot be amplified as such. If a set of complementary groups for each 'letter' of the foldamer alphabet exist and are also polymerizable, mutual template-directed polymerization and amplification is conceivable if a polymerase capable of directing this exists. In lieu of this, other informational tags can be used to obtain

the needed foldamer sequence, as detailed in Chapter 8 of *Searching for Molecular Solutions*.

General References (with hyperlinks) :

1. Vogel, C., Berzuini, C., Bashton, M., Gough, J. & Teichmann, S. A. Supra-domains: evolutionary units larger than single protein domains. [*J Mol Biol* **336**, 809-823 \(2004\).](#)
2. Berman, H., Henrick, K. & Nakamura, H. Announcing the worldwide Protein Data Bank. [*Nat Struct Biol* **10**, 980 \(2003\).](#)
3. Vitagliano, L., Masullo, M., Sica, F., Zagari, A. & Bocchini, V. The crystal structure of *Sulfolobus solfataricus* elongation factor 1alpha in complex with GDP reveals novel features in nucleotide binding and exchange. [*Embo J* **20**, 5305-5311 \(2001\).](#)
4. al-Karadaghi, S., Aevansson, A., Garber, M., Zheltonosova, J. & Liljas, A. The structure of elongation factor G in complex with GDP: conformational flexibility and nucleotide exchange. [*Structure* **4**, 555-565 \(1996\).](#)
5. Moreland, J. L., Gramada, A., Buzko, O. V., Zhang, Q. & Bourne, P. E. The Molecular Biology Toolkit (MBT): a modular platform for developing molecular visualization applications. [*BMC Bioinformatics* **6**, 21 \(2005\).](#)
6. Wagner, H. & Bauer, S. All is not Toll: new pathways in DNA recognition. [*J Exp Med* **203**, 265-268 \(2006\).](#)
7. Rudolph, M. G., Stanfield, R. L. & Wilson, I. A. How TCRs bind MHCs, peptides, and coreceptors. [*Annu Rev Immunol* **24**, 419-466 \(2006\).](#)
8. Ding, Y. H., Smith, K. J., Garboczi, D. N., Utz, U., Biddison, W. E. & Wiley, D. C. Two human T cell receptors bind in a similar diagonal mode to the HLA-A2/Tax peptide complex using different TCR amino acids. [*Immunity* **8**, 403-411 \(1998\).](#)
9. Borbulevych, O. Y., Insaiddo, F. K., Baxter, T. K., Powell, D. J., Jr., Johnson, L. A., Restifo, N. P. & Baker, B. M. Structures of MART-126/27-35 Peptide/HLA-A2 complexes reveal a remarkable disconnect between antigen structural homology and T cell recognition. [*J Mol Biol* **372**, 1123-1136 \(2007\).](#)
10. Beltrami, A., Rossmann, M., Fiorillo, M. T., Paladini, F., Sorrentino, R., Saenger, W., Kumar, P., Ziegler, A. & Uchanska-Ziegler, B. Citrullination-dependent differential presentation of a self-peptide by HLA-B27 subtypes. [*J Biol Chem* **283**, 27189-27199 \(2008\).](#)
11. Lubkowski, J., Hennecke, F., Pluckthun, A. & Wlodawer, A. The structural basis of phage display elucidated by the crystal structure of the N-terminal domains of g3p. [*Nat Struct Biol* **5**, 140-147 \(1998\).](#)
12. Marvin, D. A. Filamentous phage structure, infection and assembly. [*Curr Opin Struct Biol* **8**, 150-158 \(1998\).](#)
13. Deng, L. W. & Perham, R. N. Delineating the site of interaction on the pIII protein of filamentous bacteriophage fd with the F-pilus of *Escherichia coli*. [*J Mol Biol* **319**, 603-614 \(2002\).](#)

14. van Pouderooyen, G., Eggert, T., Jaeger, K. E. & Dijkstra, B. W. The crystal structure of *Bacillus subtilis* lipase: a minimal alpha/beta hydrolase fold enzyme. [*J Mol Biol* **309**, 215-226 \(2001\).](#)
15. Acharya, P., Rajakumara, E., Sankaranarayanan, R. & Rao, N. M. Structural basis of selection and thermostability of laboratory evolved *Bacillus subtilis* lipase. [*J Mol Biol* **341**, 1271-1281 \(2004\).](#)
16. Kawasaki, K., Kondo, H., Suzuki, M., Ohgiya, S. & Tsuda, S. Alternate conformations observed in catalytic serine of *Bacillus subtilis* lipase determined at 1.3 Å resolution. [*Acta Crystallogr D Biol Crystallogr* **58**, 1168-1174 \(2002\).](#)
17. Guex, N. & Peitsch, M. C. SWISS-MODEL and the Swiss-PdbViewer: an environment for comparative protein modeling. [*Electrophoresis* **18**, 2714-2723 \(1997\).](#)
18. Lang, D., Thoma, R., Henn-Sax, M., Sterner, R. & Wilmanns, M. Structural evidence for evolution of the beta/alpha barrel scaffold by gene duplication and fusion. [*Science* **289**, 1546-1550 \(2000\).](#)
19. Wierenga, R. K. The TIM-barrel fold: a versatile framework for efficient enzymes. [*FEBS Lett* **492**, 193-198 \(2001\).](#)
20. Galperin, M. Y., Walker, D. R. & Koonin, E. V. Analogous enzymes: independent inventions in enzyme evolution. [*Genome Res* **8**, 779-790 \(1998\).](#)
21. Varghese, J. N., Garrett, T. P., Colman, P. M., Chen, L., Hoj, P. B. & Fincher, G. B. Three-dimensional structures of two plant beta-glucan endohydrolases with distinct substrate specificities. [*Proc Natl Acad Sci U S A* **91**, 2785-2789 \(1994\).](#)
22. Hahn, M., Olsen, O., Politz, O., Borriss, R. & Heinemann, U. Crystal structure and site-directed mutagenesis of *Bacillus macerans* endo-1,3-1,4-beta-glucanase. [*J Biol Chem* **270**, 3081-3088 \(1995\).](#)
23. Subramanya, H. S., Doherty, A. J., Ashford, S. R. & Wigley, D. B. Crystal structure of an ATP-dependent DNA ligase from bacteriophage T7. [*Cell* **85**, 607-615 \(1996\).](#)
24. Shi, H. & Moore, P. B. The crystal structure of yeast phenylalanine tRNA at 1.93 Å resolution: a classic structure revisited. [*Rna* **6**, 1091-1105 \(2000\).](#)
25. Wang, L., Xie, J. & Schultz, P. G. Expanding the genetic code. [*Annu Rev Biophys Biomol Struct* **35**, 225-249 \(2006\).](#)
26. Xie, J. & Schultz, P. G. A chemical toolkit for proteins--an expanded genetic code. [*Nat Rev Mol Cell Biol* **7**, 775-782 \(2006\).](#)
27. Murray, J. B., Szoke, H., Szoke, A. & Scott, W. G. Capture and visualization of a catalytic RNA enzyme-product complex using crystal lattice trapping and X-ray holographic reconstruction. [*Mol Cell* **5**, 279-287 \(2000\).](#)
28. Flinders, J., DeFina, S. C., Brackett, D. M., Baugh, C., Wilson, C. & Dieckmann, T. Recognition of planar and nonplanar ligands in the malachite green-RNA aptamer complex. [*ChemBiochem* **5**, 62-72 \(2004\).](#)
29. Braden, B. C., Souchon, H., Eisele, J. L., Bentley, G. A., Bhat, T. N., Navaza, J. & Poljak, R. J. Three-dimensional structures of the free and the antigen-complexed Fab from monoclonal anti-lysozyme antibody D44.1. [*J Mol Biol* **243**, 767-781 \(1994\).](#)

30. Hu, S., Zhu, Z., Li, L., Chang, L., Li, W., Cheng, L., Teng, M. & Liu, J. Epitope mapping and structural analysis of an anti-ErbB2 antibody A21: Molecular basis for tumor inhibitory mechanism. [*Proteins* **70**, 938-949 \(2008\).](#)
31. Stanfield, R. L., Dooley, H., Verdino, P., Flajnik, M. F. & Wilson, I. A. Maturation of shark single-domain (IgNAR) antibodies: evidence for induced-fit binding. [*J Mol Biol* **367**, 358-372 \(2007\).](#)
32. De Genst, E., Silence, K., Decanniere, K., Conrath, K., Loris, R., Kinne, J., Muyldermans, S. & Wyns, L. Molecular basis for the preferential cleft recognition by dromedary heavy-chain antibodies. [*Proc Natl Acad Sci U S A* **103**, 4586-4591 \(2006\).](#)
33. Binz, H. K., Amstutz, P., Kohl, A., Stumpp, M. T., Briand, C., Forrer, P., Grutter, M. G. & Pluckthun, A. High-affinity binders selected from designed ankyrin repeat protein libraries. [*Nat Biotechnol* **22**, 575-582 \(2004\).](#)
34. Wahlberg, E., Lendel, C., Helgstrand, M., Allard, P., Dincbas-Renqvist, V., Hedqvist, A., Berglund, H., Nygren, P. A. & Hard, T. An affibody in complex with a target protein: structure and coupled folding. [*Proc Natl Acad Sci U S A* **100**, 3185-3190 \(2003\).](#)
35. Chu, R., Takei, J., Knowlton, J. R., Andrykovitch, M., Pei, W., Kajava, A. V., Steinbach, P. J., Ji, X. & Bai, Y. Redesign of a four-helix bundle protein by phage display coupled with proteolysis and structural characterization by NMR and X-ray crystallography. [*J Mol Biol* **323**, 253-262 \(2002\).](#)
36. Ku, J. & Schultz, P. G. Alternate protein frameworks for molecular recognition. [*Proc Natl Acad Sci U S A* **92**, 6552-6556 \(1995\).](#)
37. Dickinson, C. D., Veerapandian, B., Dai, X. P., Hamlin, R. C., Xuong, N. H., Ruoslahti, E. & Ely, K. R. Crystal structure of the tenth type III cell adhesion module of human fibronectin. [*J Mol Biol* **236**, 1079-1092 \(1994\).](#)
38. Xu, L., Aha, P., Gu, K., Kuimelis, R. G., Kurz, M., Lam, T., Lim, A. C., Liu, H., Lohse, P. A., Sun, L., Weng, S., Wagner, R. W. & Lipovsek, D. Directed evolution of high-affinity antibody mimics using mRNA display. [*Chem Biol* **9**, 933-942 \(2002\).](#)
39. Skerra, A. Imitating the humoral immune response. [*Curr Opin Chem Biol* **7**, 683-693 \(2003\).](#)
40. Skerra, A. Alternative non-antibody scaffolds for molecular recognition. [*Curr Opin Biotechnol* **18**, 295-304 \(2007\).](#)